This is a repository copy of *Detection prospects of light NMSSM Higgs pseudoscalar via cascades of heavier scalars from vector boson fusion and Higgs-strahlung*.

White Rose Research Online URL for this paper:
http://eprints.whiterose.ac.uk/108464/

Version: Accepted Version

arXiv:1503.04228v1 [hep-ph] 13 Mar 2015

Detection prospects of light NMSSM Higgs pseudoscalar via cascades of heavier scalars from vector boson fusion and Higgs-strahlung

N-E. Bomark,[a] **S. Moretti,**[b] **and L. Roszkowski**[a,1]

[a]*National Centre for Nuclear Research, Hoża 69, 00-681 Warsaw, Poland*

[b]*School of Physics & Astronomy, University of Southampton, Southampton SO17 1BJ, UK*

E-mail: Nbomark@fuw.edu.pl, S.Moretti@soton.ac.uk, L.Roszkowski@sheffield.ac.uk

ABSTRACT: A detection at the Large Hadron Collider of a light Higgs pseudoscalar would be a smoking gun signature of non-minimal supersymmetry. In this work in the framework of the Next-to-Minimal Supersymmetric Standard Model we focus on vector boson fusion and Higgs-strahlung production of heavier scalars that subsequently decay into pairs of light pseudoscalars. We demonstrate that these channels are viable for the detection of light pseudoscalars over a large part of parameter space and can serve as an important complementary mode to the dominant gluon-fusion production mode. For the singlet dominated scalar this may be the only way to measure its couplings to gauge bosons. Especially promising are channels where the initial scalar is radiated off a W as these events have relatively high rates and provide substantial background suppression due to leptons from the W. We identify three benchmark points that well represent the above scenarios. Assuming that the masses of the scalars and pseudoscalars are already measured in the GF channel allows one to constrain event kinematics, hence significantly improving detection prospects, especially in the Higgs-strahlung channels with rather heavy scalars, resulting in possible detection at 200/fb for large parts of parameter space.

---

[1]On leave of absence from the University of Sheffield, U.K.

Contents

1 Introduction

The presence of an extra singlet superfield in the Next-to-Minimal Supersymmetric Standard Model (NMSSM) (see, e.g., [1] for a review) as compared to the MSSM, has a significant impact on the ensuing phenomenology of the Higgs sector at the Large Hadron Collider (LHC). In particular, the NMSSM Higgs sector is enlarged by two neutral mass eigenstates, one scalar and one pseudoscalar, in addition to the three MSSM-like ones.[1] The singlet nature of the scalar component of the additional superfield allows its associated physical states H_1 and A_1 to be very light, even down to a few GeV, without entering into conflict with current theoretical and experimental constraints. This is so because their couplings to the fermions and gauge

---

[1]Hereafter, our book-keeping of the physical Higgs states of the NMSSM will be as follows: the CP-even states will be denoted by H_i (with $i = 1, 2, 3$ and such that $m_{H_1} < m_{H_2} < m_{H_3}$) while the CP-odd ones by A_i (with $i = 1, 2$ and such that $m_{A_1} < m_{A_2}$).

bosons of the SM are typically much smaller than those of the doublet-dominated Higgs bosons ($H_{2,3}$ and A_2), which are assumed heavier. As a consequence, the observation of any of these potentially light states, in addition to the SM-like Higgs boson already discovered at the LHC [2, 3], would constitute a hallmark signature of a non-minimal nature of supersymmetry (SUSY). Careful examination of their mass and coupling values in relation to the mass and coupling measurements of the 125 GeV SM-like Higgs boson (and possible other discovered Higgs states) in a variety of production and decay channels will eventually enable one to profile their possible NMSSM nature.

The lightest pseudoscalar A_1, in particular, can the most crucial probe of the NMSSM as it can be very light, so that in principle it is accessible in meson decays, where it has been searched for initially [4–9]. The A_1 state with mass $\gtrsim 5\,\mathrm{GeV}$ has also been probed in the possible decay of a heavy (SM-like or not) scalar Higgs boson at LEP2 [10, 11] and Tevatron [12], where no significant excess was observed. Regarding the LHC, the situation is as follows. CMS searched for a light pseudoscalar produced either singly [13] or in pairs from the decays of a non-SM-like Higgs boson [14] and decaying into the $\mu^+\mu^-$ channel, while the $A_1 A_1 \to 4\tau$ signature (via a SM-like Higgs decay) is currently under investigation [15].[2] As for ATLAS, relevant analyses include a search for scalar particles decaying via narrow resonances into two photons in the mass range above 65 GeV [18].

In addition, there are plenty of phenomenological analyses aiming at assessing the scope of A_1 discovery within the NMSSM at the LHC. Prior to the SM-like Higgs boson discovery, quite some effort was put into extending the so-called 'no-lose theorem' of the MSSM — stating that at least one Higgs boson of the MSSM would have been discovered at the LHC via the usual SM-like production and decay channels throughout the entire MSSM parameter space [19] (see [20] for a recent review) to the case of the NMSSM [21–36]. In light of the recent Higgs boson discovery though, the above theorem is necessarily verified and, if one wants to prove the NMSSM to be a viable alternative to the MSSM, one ought to probe it away from the MSSM limit.

Following this line of reasoning, if one abandons the limiting case of SM-like decay channels of Higgs states, the NMSSM offers interesting signatures which are precluded in the MSSM after the latest experimental constraints, in the form of a variety of Higgs $\to$ Two-Higgs and Higgs $\to$ Gauge-Higgs decays. A large volume of phenomenological literature exists on these topologies, claiming that, for certain NMSSM parameter choices, these would be accessible at the LHC, eventually enabling one to disentangle the NMSSM from the MSSM hypothesis, thereby establishing a so-to-say 'more-to-gain' theorem [31]. The importance of such decays in the context of the NMSSM has been emphasised in Refs. [37–39] from the point of view of fine-tuning as well as a distinctive NMSSM signature at colliders. In particular, the $H_{1,2} \to A_1 A_1$ mode has received much attention. This decay can in fact be dominant in large regions of the NMSSM parameter space. It was realised that vector boson fusion (VBF) could be a viable

---

[2]The sensitivity of the di-photon sample to a singly produced Higgs boson (of mass 150 GeV and above) decaying to $\gamma\gamma$ has also been investigated by CMS [16] alongside that of the $4b$ sample to pair production of 125 GeV Higgs bosons [17].

production channel to detect the above modes at the LHC, in which the CP-odd Higgs pair decays into $jj\tau^+\tau^-$ [24, 25, 40] (where j represents a jet). Some scope could also be afforded by a 4τ signature in both VBF and Higgs-strahlung (HS) off-gauge bosons [28]. The gluon-fusion (GF) channel too could be a means of accessing $H_1 \to A_1 A_1$ decays, as long as the light CP-odd Higgs states both decay into four muons [30] or two muons and two taus [41]. Finally, the scope of NMSSM neutral Higgs boson production in association with $b\bar{b}$ pairs was assessed in [22, 23, 33, 42–44], including the case of $H_2 \to ZA_1$ decays with $Z \to jj$ and $A_1 \to \tau^+\tau^-$.

All the above mentioned analyses were, however, performed prior to the discovery of the Higgs boson at the LHC [2, 3]. In the aftermath of the discovery, detection prospects of all NMSSM Higgs bosons, including also via their decays into other Higgs states, were recently investigated in [45], though limited to the case of inclusive rates. Further, in [46], the $A_1 \to \gamma\gamma$ decay channel was studied in the regime of a light A_1. In [47] it was then noted that in the NMSSM the A_1 could in fact be degenerate in mass with the SM-like Higgs boson $H_{\rm SM}$. It could thus cause an enhancement in the Higgs boson signal rates near 125 GeV in the $\gamma\gamma$, $b\bar{b}$ and $\tau^+\tau^-$ channels simultaneously, provided that it is produced in association with a $b\bar{b}$ pair. The $b\bar{b}A_1$ channel was also studied in detail in [48], with a more optimistic conclusion as compared to [49] for this channel. In [50] the $H_{\rm SM} \to A_1 A_1 \to 4\ell$ (with ℓ denoting $e^\pm$ and $\mu^\pm$) process at the LHC was studied in detail, while the $b\bar{b}\mu\mu$ final state was deemed the most promising in [51]. The production of A_1 via neutralino decays has also been recently revisited in [52–54]. Finally, NMSSM benchmark proposals capturing much of this phenomenology exist in the literature [35, 55].

In this work we continue to pursue a recently started endeavour [49], with an intention to systematically analyse all the production and decay processes that could potentially lead to the detection of a light NMSSM A_1 at the LHC with $\sqrt{s} = 14\,{\rm TeV}$. In [49] (see also [56, 57]), we considered the case of the light pseudoscalar A_1 produced from a heavy Higgs boson coming from GF which then decays into either A_1 pairs or ZA_1 (with the Z in turn decaying into electrons/muons). We found that the A_1 can be accessible through a variety of signatures proceeding via $A_1 \to \tau^+\tau^-$ and/or $b\bar{b}$, the former assuming hadronic decays and the latter two b-tags within a fat jet or two separate slim ones. Some of these channels were also studied in the comprehensive review of exotic Higgs decays contained in [58].

In the present paper, working under the assumption that a light A_1 state has been found through one or more of the decay channels analysed in [49], we assess the scope of the LHC Run II in profiling its nature by resorting instead to the VBF and HS Higgs production modes. This would then enable access to the heavy Higgs couplings to both charged and neutral gauge bosons, thus complementing the GF channel which only allows one to measure their fermion couplings. It is worth emphasising that for the non-SM-like scalars, this might be the only chance to access these couplings as the decay to pairs of pseudoscalars can be completely dominating. Furthermore, although the VBF and HS channels have significantly smaller cross sections than GF, the improved possibilities for tagging through the additional (forward/backward) jets for VBF and the additional leptons from vector boson decays in HS, may still render them competitive against GF, for which many of the triggers needed for fully

hadronic final states have been scarcely tested in the experimental environment.

Before plunging into the details of this new analysis, we should also point out here that in the NMSSM both H_1 and H_2, the lightest and next-to-lightest CP-even Higgs bosons, respectively, can alternatively play the role of the SM-like Higgs boson $H_{\rm SM}$, as emphasised already in [59–63] and confirmed in [49, 56, 57].

The article is organised as follows. In section 2, we define the parameter space of the NMSSM under consideration. In section 3 we explain our approach to scan the NMSSM parameter space while in section 4 we describe our signal-to-background analyses. Then in sections 5, 6 and 7 we discuss in detail our results for VBF and HS (the latter separately for the neutral (ZH) and charged (WH) channels). Finally, after presenting some benchmark points available for experimental investigation in section 8, we summarise and conclude in section 9.

2 The NMSSM parameter space

The idea behind the inclusion of an extra singlet superfield is to explain the peculiar feature of the MSSM that the supersymmetry preserving μ term is phenomenologically required to be of the same scale as the soft supersymmetry breaking mass parameters, while in principle it would be expected to be of a completely different origin.

In the NMSSM this so-called μ problem is solved by introducing an extra gauge-singlet chiral superfield $\widehat{S}$ whose scalar component receives a vacuum expectation value (VEV) due to its soft supersymmetry breaking terms. All that is needed to generate an effective μ term of the same order as the soft supersymmetry-breaking parameters, is then to have a term $\lambda\widehat{S}\widehat{H}_u\widehat{H}_d$ in the superpotential and the (effective) μ term $\mu_{\rm eff} \equiv \lambda s$ will be given by the VEV of S times the coupling constant λ. We also need to add a cubic term in $\widehat{S}$ to the superpotential, so that the terms involving $\widehat{S}$ read

$$\lambda\widehat{S}\widehat{H}_u\widehat{H}_d + \frac{\kappa}{3}\widehat{S}^3, \tag{2.1}$$

where λ and κ are dimensionless coupling constants. Further, one needs to add the corresponding soft supersymmetry breaking terms in the scalar potential. The soft supersymmetry breaking terms relevant for the Higgs sector are:

$$m_{H_u}^2|H_u|^2 + m_{H_d}^2|H_d|^2 + m_S^2|S|^2 + (\lambda A_\lambda SH_uH_d + \frac{\kappa}{3}A_\kappa S^3 + h.c.), \tag{2.2}$$

where m_{H_u}, m_{H_d}, m_S, A_λ and A_κ are dimensionful mass and trilinear parameters. By minimising the scalar potential we can trade the three scalar mass parameters for κ, $\mu_{\rm eff}$ and $\tan\beta$ (i.e., the ratio between the VEVs in the up type and down type Higgs doublets, v_u/v_d).

Throughout this paper we use parameters defined at the Grand Unification Theory (GUT) scale. For the sfermion masses we use a common mass parameter m_0 and for all gaugino masses we use a common parameter $m_{1/2}$. Similarly, we use a common parameter A_0 for all trilinear parameters except A_λ and A_κ. Since these parameters should not affect the Higgs sector very much, unifying them in the above manner allows for maximum freedom in the Higgs sector

while keeping the number of free parameters at a manageable level. This leaves us with nine parameters (as mentioned, defined at the GUT scale):

$$m_0, \ m_{1/2}, \ A_0, \ \tan\beta, \ \mu_{\mathrm{eff}}, \ \lambda, \ \kappa, \ A_\lambda, \ A_\kappa. \tag{2.3}$$

As can be seen in the tree-level mass expression for H_{SM} (i.e. the lightest doublet dominated scalar, either H_1 or H_2) in the NMSSM [1],

$$m_{H_{\mathrm{SM}}}^2 \simeq m_Z^2 \cos^2 2\beta + \lambda^2 v^2 \sin^2 2\beta - \frac{\lambda^2 v^2}{\kappa^2} \left[\lambda - \sin 2\beta \left(\kappa + \frac{A_\lambda}{2s} \right) \right]^2, \tag{2.4}$$

there is an additional contribution to the Higgs mass coming from the λ term, not present in the MSSM. This means that, when this term is sizable, i.e., when λ is large and $\tan\beta$ is small, one can obtain the measured 125 GeV mass without resorting to large radiative corrections from the stop sector, which is necessary in the MSSM. In the forthcoming sections we will refer to this part of parameter space as the 'naturalness limit'. Note that in this limit it is of importance also that κ tends to be big to suppress the negative term. Finally, notice that, when $H_2 = H_{\mathrm{SM}}$, it is also possible that some mixing between H_1 and H_2 increases m_{H_2} further, hence making it even easier to achieve (and indeed exceed) the required 125 GeV [64].

3 The scans

In order to investigate the NMSSM parameter space we make use the results of the Bayesian scans from [49]. These scans used MultiNest-v2.18 [65] for nested sampling of the parameter space and NMSSMTools-v4.2.1 [66] for the calculation of the Higgs mass spectrum, couplings, Branching Ratios (BRs) and constraints on the parameter points. The output from NMSSMTools was further processed by HiggsBounds-v4.1.3 [67–70] to ensure against exclusion from searches for other Higgs bosons. Also SuperIso-v3.3 [71] was used to calculate b-physics variables. These were then required to comply with the constraints from [72]:

- $\mathrm{BR}\,(\mathrm{B_s} \to \mu^+\mu^-) = (3.2 \pm 1.35 \pm 0.32) \times 10^{-9}$, where the last quantity implies a 10% theoretical error in the numerical evaluation,

- $\mathrm{BR}\,(\mathrm{B_u} \to \tau\nu) = (1.66 \pm 0.66 \pm 0.38) \times 10^{-4}$,

- $\mathrm{BR}\,\left(\overline{\mathrm{B}} \to \mathrm{X_s}\gamma\right) = (3.43 \pm 0.22 \pm 0.21) \times 10^{-4}$.

To guard against over-closure of the Universe, an upper bound of $\Omega_\chi h^2 < 0.131$ on the dark matter relic density was also applied. This was set assuming a 10% theoretical error on the central value of 0.119 from PLANCK [73] and the relic density was calculated with the help of MicrOMEGAs-v2.4.5 [74].

The parameter ranges used in the scans are given in table 1. The reduced range focuses on the naturalness limit and, since the couplings relevant to, e.g., $H_i \to A_1 A_1$ decays depend on λ this is the most promising part of parameter space to look for these channels. Therefore

Parameter	Extended range	Reduced range
m_0 (GeV)	$200 - 4000$	$200 - 2000$
$m_{1/2}$ (GeV)	$100 - 2000$	$100 - 1000$
A_0 (GeV)	$-5000 - 0$	$-3000 - 0$
μ_{eff} (GeV)	$100 - 2000$	$100 - 200$
$\tan\beta$	$1 - 40$	$1 - 6$
λ	$0.01 - 0.7$	$0.4 - 0.7$
κ	$0.01 - 0.7$	$0.01 - 0.7$
A_λ (GeV)	$-2000 - 2000$	$-500 - 500$
A_κ (GeV)	$-2000 - 2000$	$-500 - 500$

Table 1. Parameter ranges used in the scans. The reduced range focuses on the naturalness limit.

this is the only scan used for $H_2 = H_{\mathrm{SM}}$. For $H_1 = H_{\mathrm{SM}}$, however, it turns out that only an extended scan can give any relevant points for $H_1 \to A_1 A_1$, thus, the results shown will be a superposition of the two scans.

The scans also contain a bias towards low pseudoscalar masses (favouring $m_{A_1} \lesssim 65$ GeV, but allowing m_{A_1} up to 140 GeV) and SM-like signals rates for H_{SM}. These constraints are implemented to ensure that the scans do not waste too much time exploring uninteresting parts of parameter space. Conversely, they should not exclude any points that might be of interest for further investigation.

The LHC signal rates for a scalar H_i decaying into a final state X, are parametrised as,

$$R_X \equiv \frac{\sigma(gg \to H_i) \times \mathrm{BR}(H_i \to X)}{\sigma(gg \to h_{\mathrm{SM}}) \times \mathrm{BR}(h_{\mathrm{SM}} \to X)}, \tag{3.1}$$

where h_{SM} is the Higgs boson of the SM (here assumed to have the same mass as the H_i it is being compared to). These are used as good approximations for the inclusive signal rates,

$$\mu_X = \frac{\sigma(pp \to H_i \to X)}{\sigma(pp \to h_{\mathrm{SM}} \to X)}. \tag{3.2}$$

In order to be consistent with experiments we use the measured signal rates from CMS [75],

$$\mu_{\gamma\gamma} = 1.13 \pm 0.24, \quad \mu_{ZZ} = 1.0 \pm 0.29, \tag{3.3}$$

and ATLAS[3] [79],

$$\mu_{\gamma\gamma} = 1.57^{+0.33}_{-0.28}, \quad \mu_{ZZ} = 1.44^{+0.40}_{-0.35}, \tag{3.4}$$

---

[3]Note that ATLAS has released improved limits for both $\mu_{\gamma\gamma}$ [76], μ_{ZZ} [77] and μ_{WW} [78], also providing separate limits for GF production. However, to be able to compare more directly to the results of [49], we keep the previous constraints. Using the new constraints would mostly make the ATLAS sample look more similar to the CMS ones as the new limits are more SM-like (apart from some rather peculiar behaviour of μ_{ZZ} from GF production). Finally, there is also the point that, with the old constraints, the old ATLAS sample can serve as an illustration of what rates higher than the SM values would imply for our detection prospects.
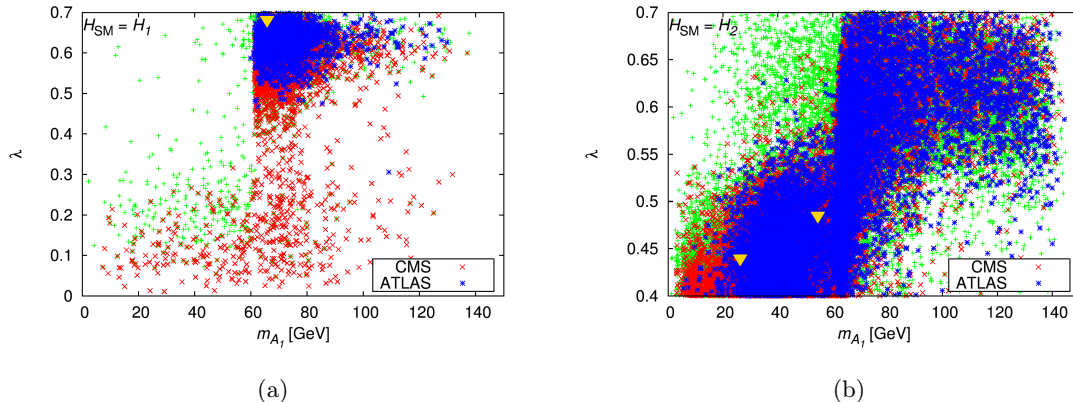
Figure 1. The parameters λ versus m_{A_1}. The red points are consistent with CMS measurements of μ_{ZZ} and $\mu_{\gamma\gamma}$ while the blue points are compatible with ATLAS data. The green points are only kept for reference as they are excluded by both experiments. The golden triangles mark the benchmark points defined in section 8.

to split our parameter points into three different samples: one consistent with CMS, one consistent with ATLAS and the remaining points (consistent with neither), which are kept for reference. For all samples we require $m_{H_{SM}}$ to lie between 122 and 129 GeV. The best experimental values of the Higgs mass are 125.03 GeV from CMS [75] and 125.36 GeV from ATLAS [80] with uncertainties of the scale of a fraction of a GeV, however, to allow for potentially large theoretical uncertainties, we allow a significantly larger range. Note, though, that the benchmark points of section 8 are within the experimental limits.

In figure 1 we plot λ against m_{A_1} for both $H_1 = H_{SM}$ and $H_2 = H_{SM}$. In figure 1(a) we see that there are very few points with m_{A_1} below $m_{H_1}/2$. This is because of the bias towards SM-like signal rates imposed on H_1; if $m_{A_1} < m_{H_1}/2$ the $H_1 \to A_1 A_1$ channel is open and, as long as λ is fairly large, tends to dominate the decays of H_1, thus strongly reducing R_{ZZ} and $R_{\gamma\gamma}$, and ultimately rendering the points incompatible with both CMS and ATLAS. This is further emphasised by the fact that some of the excluded (green) points do appear in the very low mass and high λ region, but none of the CMS (red) or ATLAS (blue) points do. In the extended scan, CMS data allow some points with low λ to have rather low m_{A_1} but this is not possible for the ATLAS data as $\mu_{\gamma\gamma}$ and μ_{ZZ} are higher.

Looking at figure 1(b) we see that the situation for $H_2 = H_{SM}$ is somewhat different. Since the Higgs mass requirement is easier to meet here, the parameter space is less constrained and there is a substantial number of points compatible with both CMS and ATLAS, below $m_{H_2}/2$. Though λ does not reach its upper limit below $m_{H_2}/2$, it is clearly larger for these points than for the corresponding CMS points in the $H_1 = H_{SM}$ case.

Finally, in both figure 1(a) and (b), there is a depletion of points above 70–80 GeV: this is due to the bias towards low m_{A_1} included in the scans.
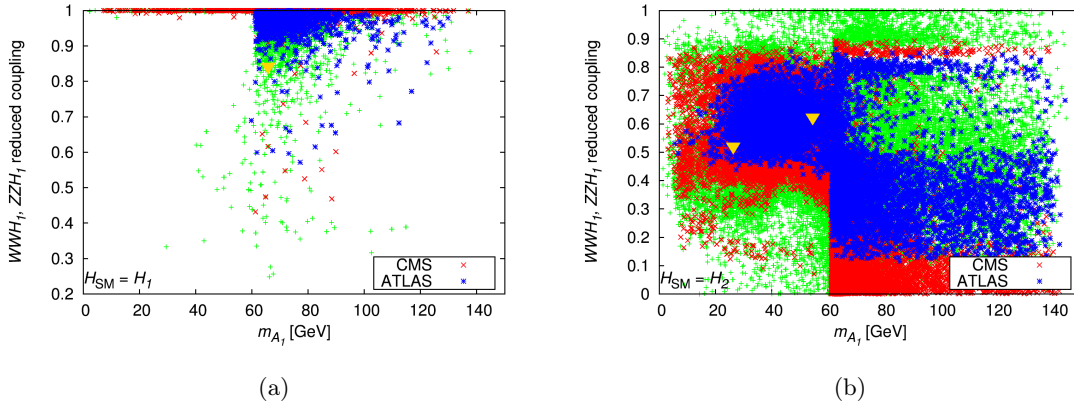
Figure 2. Reduced couplings to WW and ZZ pairs for H_1. The colour code for the points is the same as in figure 1.

As the relevant couplings for both VBF and HS are the WWH and ZZH couplings, we show in figures 2 to 4 the corresponding reduced couplings for H_1 (figure 2), H_2 (figure 3) and H_3 (figure 4) for both the $H_1 = H_{SM}$ (figure 2 to 4, plots labelled (a)) and the $H_2 = H_{SM}$ (figure 2 to 4, plots labelled (b)) case. For both H_1 and H_2 these can take values up to one but not so for H_3.

To understand this let us look at the couplings of interest: they both have a factor [1]

$$(v_d S_{31} + v_u S_{32}), \tag{3.5}$$

where S_{31} and S_{32} are elements of the neutral scalar mixing matrix. We know that $v_u/v_d = \tan\beta$ by definition and, due to the structure of the mixing matrices, it turns out that $S_{31}/S_{32} \approx -\tan\beta$. Hence the factor (3.5) becomes small, from figure 4 we see that this reduced coupling tends to be ≈ 0.01 or smaller and, since it comes squared in the production cross sections for both VBF and HS, we get a suppression factor of at least 10^{-4}, rendering these channels useless for H_3. In contrast, for both H_1 and H_2, the coupling strength can be sizable.

4   Event analyses

Since the vector boson couplings to H_3 are always very small we do not consider channels including H_3 production here, they do not have big enough cross sections to be of any interest. Furthermore, since the channels $H_{1,2} \to A_1 Z$ were shown in [49] to be very difficult, we here focus only on the $H_{1,2} \to A_1 A_1$ channels. Given the lower cross sections for VBF and HS production as compared to GF, none of the other channels carry promise for detection.

To estimate the sensitivity in the channels of interest we use MadGraph5_aMC@NLO [81], employing default parton distribution functions and factorisation and renormalisation scales, to generate the relevant backgrounds. Hadronisation and signal generation is then done using Pythia 8.180 [82], while jet clustering and jet substructure studies are done using FastJet-v3.0.6 [83].
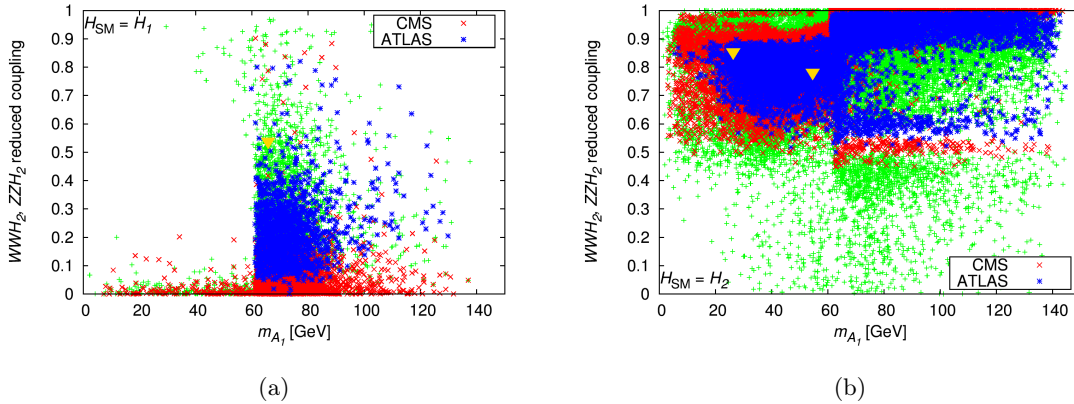
Figure 3. Reduced couplings to WW and ZZ pairs for H_2. The colour code for the points is the same as in figure 1.

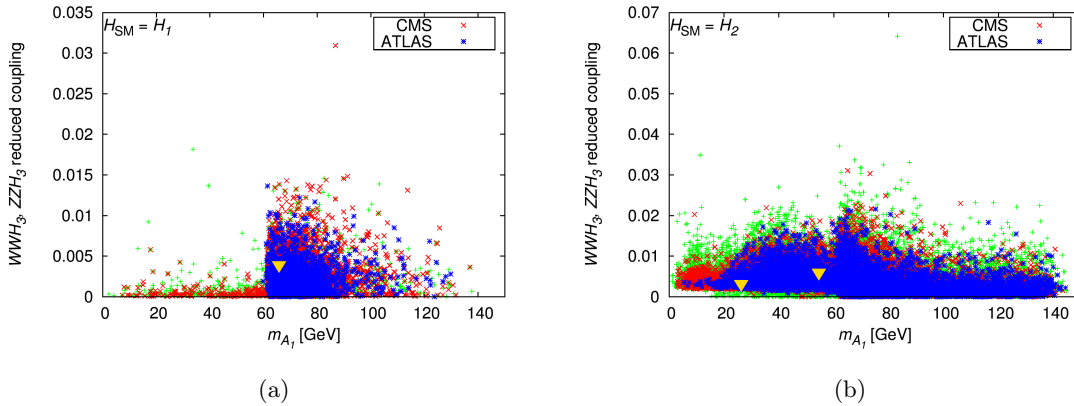**Figure 4**. Reduced couplings to WW and ZZ pairs for H_3. The colour code for the points is the same as in figure 1.

The production cross sections for the signals are calculated using tabulated cross sections for the SM Higgs, taken from [84], together with reduced couplings for the relevant scalar from NMSSMTools.

For all final state objects we use the following acceptance cuts:

- $|\eta| < 2.5$ for all final state objects,

- $p_T > 15\,\text{GeV}$ far all final state jets (τ-jets, b-jet and light jets),

- $p_T > 10\,\text{GeV}$ far all final state leptons ($e^\pm$, $\mu^\pm$),

- $\Delta R \equiv \sqrt{(\Delta\eta)^2 + (\Delta\phi)^2} > 0.2$ for all b-quark pairs,

- $\Delta R > 0.4$ for all other pairs of final state objects,

Channel	Parton level cross section
VBF	
$2j + 4b$	72 pb
$2j + 2b2\tau$	0.19 pb
$2j + t\bar{t}$	80 pb
ZH	
$Z + 4b$	0.31 pb
$Z + 2b2\tau$	2.7 fb
WH	
$W + 4b$	36 fb
$t\bar{t}b\bar{b}$	4.0 pb
$t\bar{t}$	597 pb

Table 2. Background cross sections for the dominant backgrounds at parton level as calculated by MadGraph.

where p_T, η, ϕ are the transverse momentum, pseudorapidity and azimuthal angle, respectively. The tagging efficiency is taken to be 50% for both b and τ jets and we assume no knowledge about the charge of the jets. For the $t\bar{t}$ background for the WH channel, we assume a 1% mistagging probability for light jets.

For the VBF backgrounds the two additional light jets are required to satisfy the following criteria:

- $|\eta| < 5$,

- $p_T > 30\,\text{GeV}$,

- $\Delta R > 3$,

- $M_{jj} > 300$ GeV,

where M_{jj} is the invariant mass of the two forward/backward jets. (Due to numerical difficulties in producing enough statistics, somewhat harder cuts, $M_{jj} > 500$ GeV and $p_T > 40$ GeV, are imposed on the parton level production in the $4b$ final state.) In addition, the jets are required to be located in the opposite hemispheres (i.e. one positive and one negative η) and there should be no other jet (apart from the signal objects) with $p_T > 30$ GeV between (in terms of η) the two jets.

The cross sections for the dominant backgrounds after the above acceptance cuts are applied, are given in table 2.

In order to optimise the sensitivity to boosted A_1s we employ the jet substructure method of [85] (see also [49] for further details). This gives us fat jets that we assume to originate from an A_1 decaying into a $b\bar{b}$ pair. To avoid contamination from single b-jets, we require all fat jets to have $p_T > 30$ GeV and invariant mass > 12 GeV.

For each event with the proper final state we look for two A_1 candidates (either one fat jet, two b-jets or two τ-jets depending on which channel we are looking at) and compare their respective invariant mass: if they are within 15 GeV of each other we accept that event and if, in addition, the combined invariant mass of the two candidates is within 125 ± 30 GeV, it is accepted as an event where an H_{SM} was produced and decayed into two A_1s. In all the channels we perform two analyses in parallel: one with the jet substructure method, where only fat jets and no single b-jets are used, and one where no jet substructure is exploited but only single b-jets are used. For the four b-jet final state we check all combinations of b-jet pairs and accept the first one with both invariant masses within 15 GeV of each other.

To obtain the sensitivity for a given m_{A_1} we then count the events where the A_1 candidates masses are within 15 GeV of the mass m_{A_1} and can then calculate — for a given luminosity, $\mathcal{L}$ — how large signal cross section is needed to obtain a significance $S/\sqrt{B} > 5$ where S is the number of signal events and B is the background. In all channels we require at least 10 events in order to claim discovery, so if $S/\sqrt{B} > 5$ is fulfilled for $S < 10$, we instead use $S > 10$ as the limiting sensitivity. This means that, in channels with very low background, the sensitivity is $\propto \mathcal{L}$ rather than $\propto \sqrt{\mathcal{L}}$ as is the case for $S/\sqrt{B}$.

We will be studying the VBF and HS channels in turn, splitting the latter into the ZH and WH modes.

5   VBF

The backgrounds used in the analysis of the VBF mode are irreducible, i.e., $4b+2$ jets and $2b2\tau+2$ jets. In addition, we include the $t\bar{t}+2$ jets — with both Ws from the top quarks decaying to τs — in the $2b2\tau$ channel. Since the latter turns out to be the dominant background in this channel, we also invoke a cut on Missing Transverse Momentum (MET) to reduce it.

This cut requires that the p_T of the two τ-jets combined should be larger than the total MET of the event. This reduces the $t\bar{t}+2$ jets background by a factor 2-3 while leaving both signal and irreducible backgrounds virtually intact. Note, however, that the MET here is simply the sum of the momentum of all invisible particles (i.e., neutrinos), a full detector simulation with mis-measured/missing jets, pile-up etc. would be necessary to fully determine the true effectiveness of this cut. This latter cut, though effective, is, however, not crucial for the usefulness of this analysis.

Figure 5 shows the discovery reach in the interesting channels for 3000/fb of integrated luminosity and using the overall constraint that the total four-body invariant mass should be 125±30 GeV. It is clear that the $2b2\tau$ channels are the most promising ones and hence we will not consider the $4b$ channels in the following. All sensitivity curves have been divided by a factor 0.9 for each $b\bar{b}$ pair in the final state and a factor 0.1 for each $\tau\tau$ pair in the final state, to allow for a direct comparison of the sensitivity to $\sigma(q\bar{q} \to q\bar{q}H_i) \times \text{BR}(H_i \to A_1A_1)$. As expected, we see in figure 5 that the jet substructure analysis only works well for rather low m_{A_1}.
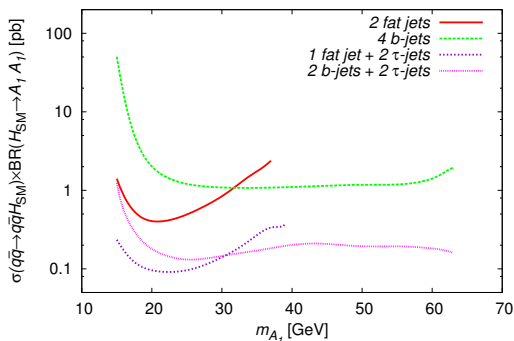
Figure 5. Sensitivity for the $4b$ and $2b2\tau$ channels in VBF production.

5.1 H_1 SM-like

To illustrate the reach of the LHC in these channels in figure 6 we compare the sensitivity with
the points from our scans when $H_1 = H_{SM}$. In figure 6(a), we show sensitivity curves using a
125 GeV Higgs (and employing the corresponding constraint), always using the best out of the
2 b-jets and fat jet analyses. As is clearly seen, the prospects for $H_1 \rightarrow A_1 A_1$ will always be
rather limited due to the small number of points in the interesting region of parameter space.
As mentioned in section 3, this is due to the difficulty in obtaining acceptable signal rates for
H_1 when the $H_1 \rightarrow A_1 A_1$ channel is open, thus highly suppressing the number of points with
$m_{A_1} < m_{H_1}/2$.

   As regards the $H_2 \rightarrow A_1 A_1$ channel, it is possible to have some more points just above the
$m_{A_1} < m_{H_1}/2$ threshold. This can be seen in figure 6(b), where the prospects for $H_2 \rightarrow A_1 A_1$
are illustrated. Figure 6(b) uses sensitivity curves for $m_{H_2} = 175$ GeV in order to cover the
whole interesting parameter space. Also, here do we always employ the analysis (with or
without jet substructure) with the best sensitivity. We see that just above the $H_1 \rightarrow A_1 A_1$
threshold there are some points within reach although they only constitute a small fraction of
parameter space.

5.2 H_2 SM-like

With $H_2 = H_{SM}$ it is significantly easier to obtain a light pseudoscalar. This means that
the prospects for detection in this case are significantly better. In figure 7(a) we show the
sensitivity for $H_1 \rightarrow A_1 A_1$, both with jet substructure using $m_{H_1} = 100$ GeV and without jet
substructure using $m_{H_1} = 125$ GeV, but without constraining the four-body invariant mass.
We use two separate curves since they use different m_{H_1}: the inclusion of both allows us to
realistically estimate the sensitivity in the whole range of m_{A_1}. Though it will require 3000/fb
to cover the whole parameter space, already 300/fb does show significant promise. However,
at low mass, even 3000/fb might not be enough.

   This can be understood by considering that, for lower m_{A_1}, also m_{H_1} tends to be smaller
and our sensitivity decreases with a lighter initial scalar. For the $4b$ final state this can be
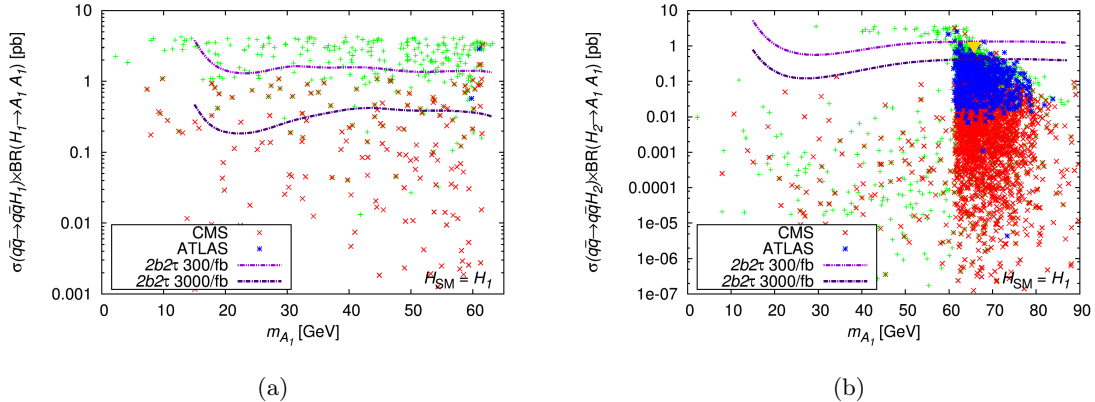
Figure 6. LHC reach in $H_1 \rightarrow A_1 A_1$ (left) and $H_2 \rightarrow A_1 A_1$ (right) for $H_1 = H_{\rm SM}$ in the VBF channel. The colour code for the points is the same as in figure 1.

compensated by an improved sensitivity due to the fat jet analysis, however, as can be seen in figure 5, the low mass improvement with the fat jet analysis is not as great for $2b2\tau$ as it is for $4b$, leading to comparatively poor sensitivity to $m_{A_1} \approx 20$ GeV in figure 7(a). It is also worth noticing a set of points around $\sigma(q\bar{q} \rightarrow q\bar{q}H_1) \times {\rm BR}(H_1 \rightarrow A_1 A_1) \approx 0.1$ pb in figure 7(a). These are points with a rather light and singlet like H_1 ($m_{H_1} \approx 40$ GeV) as well as a light $(30 - 40$ GeV) singlino. While most points with scalars, pseudoscalars and neutralinos below 60 GeV struggle to meet the signal rate requirements for the $H_{\rm SM}$ due to competing decays to scalar, pseudoscalar and neutralino pairs; as those channels tend to decrease when the masses becomes very low, this set of points survive. Moreover, due to annihilations through Z, they also provide proper relic abundance. However, as the H_1 in these points is very singlet like, the reduced coupling to vector bosons is very small (around $0.2 - 0.3$ as seen in figure 2(b)) and hence beyond reach for the channels studied here.

In figure 7(b) we show the sensitivity in the $H_2 \rightarrow A_1 A_1$ channel using $m_{H_2} = 125$ GeV and requiring the four-body invariant mass to be 125 ± 30 GeV. For all points along the sensitivity curves we use the analysis that gives the best sensitivity (with or without jet substructure). Detection at 300/fb is almost excluded by the signal rate measurements, but 3000/fb does carry some promise.

6 Higgs-strahlung via ZH

With an additional Z boson, triggering and background suppression is much improved. To extract the signal we only use leptonically decaying Z bosons. This means, that in addition to acceptances, we require one di-lepton pair with invariant mass 90 ± 10 GeV. This is very powerful in suppressing the backgrounds, however, the small leptonic BR of the Z together with the small production cross sections in the ZH channel, means that one will struggle to get a large enough signal. As one would then expect, the best final state to look for is not
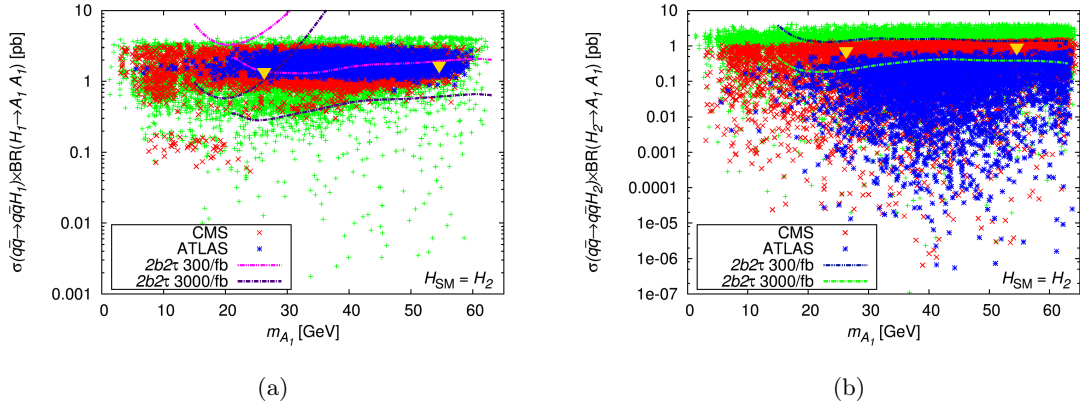
Figure 7. LHC reach in $H_1 \to A_1 A_1$ (left) and $H_2 \to A_1 A_1$ (right) for $H_2 = H_{\rm SM}$ in the VBF channel. The colour code for the points is the same as in figure 1.
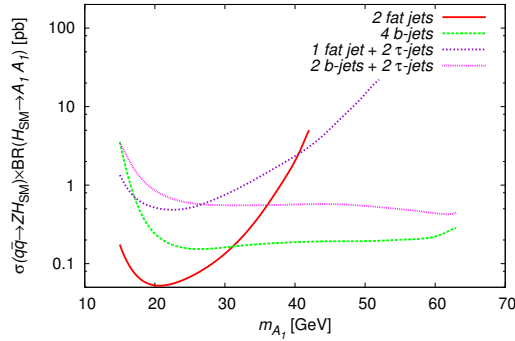

Figure 8. Sensitivity for HS off a Z boson.

$2b2\tau$ as was used before, but rather $4b$ which gives the highest signal rate. This is clearly seen in figure 8, where the sensitivity in the various channels are shown for 3000/fb of integrated luminosity. All channels use $m_{H_i} = 125$ GeV and the corresponding cut on the total final state invariant mass.

6.1 H_1 SM-like

Similarly to the VBF case, the SM-like H_1 scenario is difficult with respect to detection. In figure 9(a) we show the sensitivity in the $H_1 \to A_1 A_1$ channel, given $m_{H_1} = 125$ GeV (with a corresponding cut on the four-body invariant mass), as compared to the acceptable parameter points. We notice that the prospects are even dimmer than in the VBF case. As usual only the analysis with the best sensitivity is used in each point of the curves.

Moving on to $H_2 \to A_1 A_1$, we see in figure 9(b) that there is essentially no hope for detection even at 3000/fb. The curves here correspond to $m_{H_2} = 175$ GeV, with no cut on the total final state invariant mass.
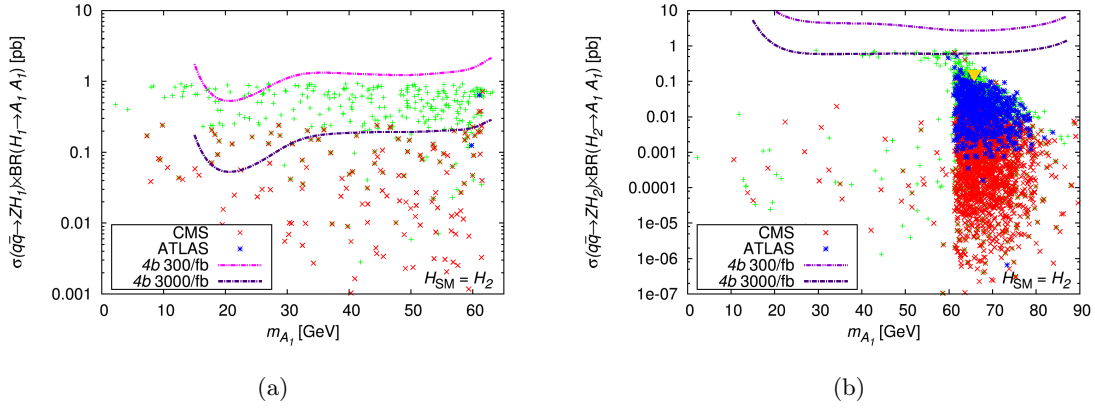
Figure 9. LHC reach in $H_1 \to A_1 A_1$ (left) and $H_2 \to A_1 A_1$ (right) for $H_1 = H_{\mathrm{SM}}$ in the ZH channel. The colour code for the points is the same as in figure 1.

Figure 10. LHC reach in $H_1 \to A_1 A_1$ (left) and $H_2 \to A_1 A_1$ (right) for $H_2 = H_{\mathrm{SM}}$ in the ZH channel. The colour code for the points is the same as in figure 1.
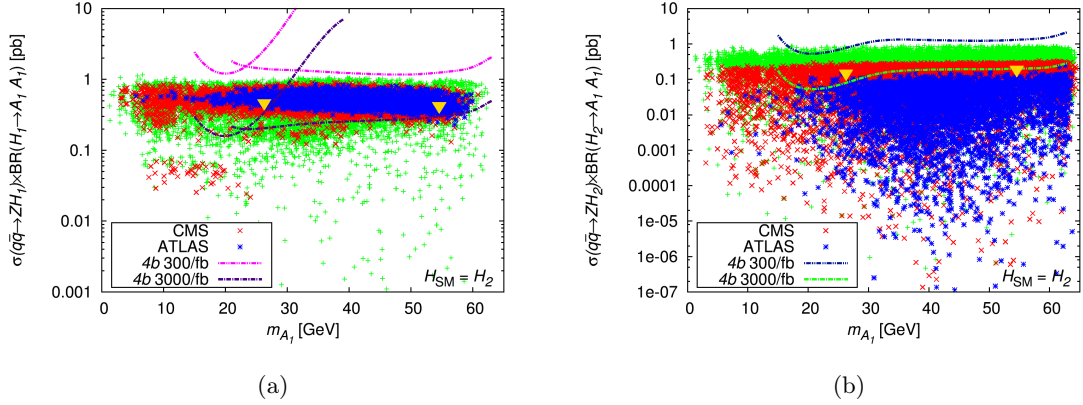
6.2 H_2 SM-like

As with VBF production, the $H_2 = H_{\mathrm{SM}}$ case offers somewhat better prospects. Though, as can be seen for $H_1 \to A_1 A_1$ in figure 10(a) — where the sensitivity curves use $m_{H_1} = 100$ GeV with jet substructure, and $m_{H_1} = 125$ GeV with single b-jets (no constraint on overall invariant mass), respectively — we will need up to 3000/fb to detect anything.

In figure 10(b) we show the reach for $H_2 \to A_1 A_1$, the sensitivity curves correspond to $m_{H_2} = 125$ GeV and the corresponding constrain on the four-body invariant mass, always showing the most sensitive analysis. At 3000/fb there is some hope for discovery but most of the parameter space remains untouched. In particular, higher signal rates in the ATLAS sample almost exclude a detection in this channel even at 3000/fb.

7   Higgs-strahlung via WH

In general WH production will have higher cross sections than ZH production and, since the W also has roughly three times higher leptonic BR as compared to the Z, this channel will exhibit much higher rates. In order to tag the W we require exactly one isolated lepton in the event, in addition to the signal objects. Similarly to ZH production, we only look at the channel with the highest rate, i.e., $W + 4b$.

There has been a number of earlier studies of the $W + 4b$ channel, including parton level studies [86] and [87] and a full detector study in [88]. While the parton level analysis of [87] arrived at significantly higher sensitivity than we did, our results are in reasonable agreement with [88]. (Note however that, although both of these studies use four b-tags as well as a cut on the four-body invariant mass, neither of them uses the requirement that both A_1 candidates should have similar mass.)

In addition to the irreducible $W + 4b$ background, there are significant backgrounds from $t\bar{t}$ — with two light jets from one of the resulting Ws being mistagged as b-jets — as well as from $t\bar{t}b\bar{b}$ events. The latter is in our studies the most significant one, often at least one order of magnitude larger than the irreducible background. This conclusion is in agreement with [87], while [88] finds that detector smearing pushes the $t\bar{t}$ background to lower invariant masses and hence becomes a significant background also at 125 GeV. To suppress the $t\bar{t}b\bar{b}$ background we employ a veto against hadronically decaying Ws. This means an event with two light jets with $p_T > 15$ GeV and combined invariant mass $= 80 \pm 15$ GeV is rejected as it is likely to come from a $t\bar{t}b\bar{b}$ event with one W decaying leptonically and the other one hadronically. The events where both Ws decay leptonically should be suppressed by the fact that we ask for exactly one lepton and hence reject events with two isolated leptons (this also suppresses any $Z + 4b$ backgrounds).

Since the smallness of the signal rates in both WH and (even more) in ZH production is a bigger problem than background suppression, one could consider requiring only three b-tags. This was the approach of [86] and should yield significantly higher signal rates, especially as one b-jet is often missed due to p_T cuts, etc. However, this requires a much more detailed study as there are many more contributing sources of background. It is also not clear how to implement the invariant mass constraints as one have to assume that sometimes the fourth b-jet is not selected even as a light jet. Such considerations are therefore beyond the scope of this paper.

7.1 H_1 SM-like

In this case higher rates as compared to ZH production does mean better discovery prospects even though the background is also larger due to $t\bar{t}b\bar{b}$.

In figure 11(a) we show the discovery reach in the $H_1 \to A_1 A_1$ channel in the $H_1 = H_{\rm SM}$ case. The sensitivity curves are set for $m_{H_1} = 125$ GeV and the corresponding cut on the overall invariant mass. If we compare with figure 9(a), the reach here is much greater, even 300/fb might be enough for detecting some A_1s around 20 GeV. Such a discovery is not
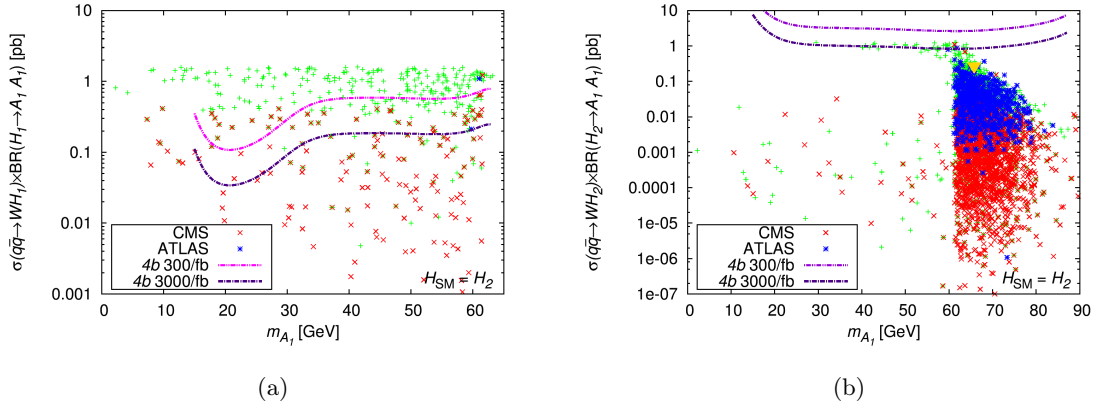
Figure 11. LHC reach in $H_1 \to A_1 A_1$ (left) and $H_2 \to A_1 A_1$ (right) for $H_1 = H_{\rm SM}$ in the WH channel. The colour code for the points is the same as in figure 1.

possible even for VBF production, as can be seen in figure 6(a), where 300/fb does not show any discovery prospects. The reason for the relative success of WH production for these low masses is that in the $4b$ final state the use of fat jets leads to a more significant improvement over a single b-jet analysis than is the case for the $2b2\tau$ channel used for VBF production.

The $H_2 \to A_1 A_1$ channel is much less optimistic, as can be seen in figure 11(b), where we set $m_{H_2} = 175$ GeV with no cut on overall invariant mass for the sensitivity curves. The almost complete absence of discoverable points even at 3000/fb is due to the fact that the $t\bar{t}b\bar{b}$ and $t\bar{t}$ backgrounds tend to grow at higher invariant masses, so that not having an overall cut on the four-body invariant mass is a serious disadvantage. One could still try some invariant mass cuts to suppress these backgrounds but we leave such considerations to section 8.

7.2 H_2 SM-like

In line with our earlier findings, the $H_2 = H_{\rm SM}$ case is much more promising. As can be seen in figure 12(a) — displaying sensitivity curves with $m_{H_1} = 100$ GeV (using fat jets) and 125 GeV (using b-jets) but with no overall cut on invariant mass — there is significant hope for detection in $H_1 \to A_1 A_1$ already at 300/fb, while 3000/fb should cover the entire parameter space. Especially noteworthy is the improved sensitivity in the low mass region as compared to VBF production. This is again a consequence of the strength of the fat jet analysis for $4b$ as well as the main backgrounds $t\bar{t}b\bar{b}$ and $t\bar{t}$ being smaller for lower invariant masses. It might even look like the inclusion of a cut on the four-b invariant mass might extend the reach to the points with $\sigma(q\bar{q} \to WH_1) \times {\rm BR}(H_1 \to A_1 A_1) \approx 0.1$ pb. However, recall that those points have $m_{H_1} \approx 40$ GeV and hence the sensitivity is significantly lower than for the curves of figure 12(a). These points are therefore truly beyond the reach of any analysis in this paper.

For $H_2 \to A_1 A_1$ (figure 12(b)) it does not look as promising as for $H_1 \to A_1 A_1$, but at 3000/fb one can cover a large part of parameter space and even 300/fb might be enough for accessing A_1 with mass around 20 GeV. Here we use $m_{H_2} = 125$ GeV and constrain the
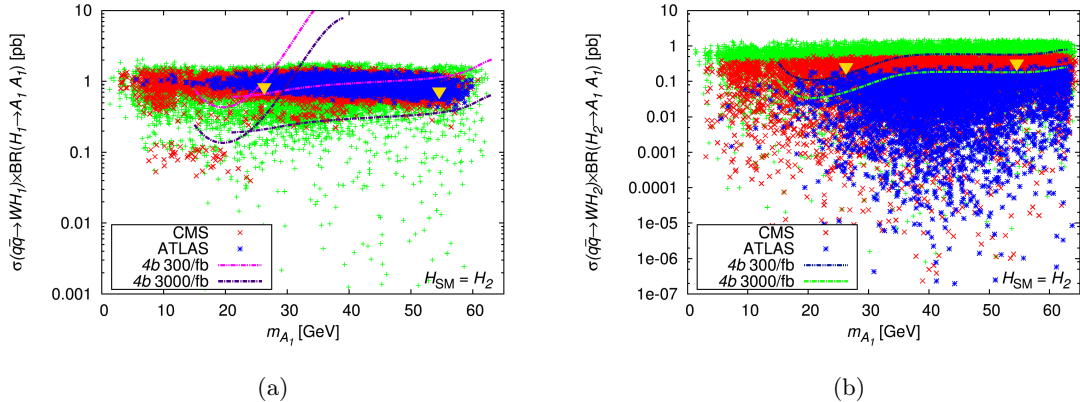
Figure 12. LHC reach in $H_1 \to A_1 A_1$ (left) and $H_2 \to A_1 A_1$ (right) for $H_2 = H_{\mathrm{SM}}$ in the WH channel. The colour code for the points is the same as in figure 1.

four-body invariant mass of the final state to be 125 ± 30 GeV. The sensitivity curves use a combination of the fat jet and the single b-jet analyses, always showing the more sensitive one.

8 Benchmark points

As mentioned before, the detection sensitivities in all the channels studied in this paper are significantly worse than the corresponding results from GF production.[4] Furthermore, this is generally true for all parameter space regions that we have been able to access in the analyses carried out here. Therefore it is fair to assume that, by the time the channels under investigation become interesting for experimental study, the lightest scalar (H_1 and H_2) as well as pseudoscalar (A_1) Higgs states will already have been discovered via GF and the goal for both the VBF and HS channels will become to enable one further study their properties, as explained in the introduction.

For this purpose we define three benchmark points and study them under the assumption that we know the masses involved and can hence use this information to further constrain the kinematics in the attempt to increase the sensitivity.[5] The details of the three points are given in table 3. The points are chosen to cover as much as possible of the interesting parameter space. Point 1 has a rather light A_1 of 26 GeV and hence lies in the region where jet substructure methods are of importance, while point 2 is closer to the threshold for $H_{1,2} \to A_1 A_1$ with $m_{A_1} = 55$ GeV. The last point is the only one with $H_1 = H_{\mathrm{SM}}$ and with $m_{A_1} = 66$ GeV, it is designed for $H_2 \to A_1 A_1$ studies. Recall that, for $H_1 = H_{\mathrm{SM}}$, this is the only part of parameter space with a significant number of promising points.

---

[4]This is true unless the triggering in the GF channel turns out to be more challenging than what is presently hoped for.

[5]Even with our prior knowledge of the masses, these analyses can be employed by scanning over the masses involved. This, however, would render large look-elsewhere effects.

Case	$H_{\mathrm{SM}} = H_2$		$H_{\mathrm{SM}} = H_1$
	Point 1	Point 2	Point 3
Input parameters			
m_0 (GeV)	1532.9	1040.0	1049.8
$m_{1/2}$ (GeV)	512.47	993.7	902.17
A_0 (GeV)	-1855.4	-2065.8	-1427.2
μ_{eff} (GeV)	127.76	117.5	186.46
$\tan\beta$	5.436	4.688	2.206
λ	0.44	0.4852	0.6824
κ	0.1856	0.2434	0.1941
A_λ (GeV)	215.57	-224.6	-410.15
A_κ (GeV)	270.27	52.77	-17.60
Observables			
m_{A_1} (GeV)	26.27	54.56	65.76
m_{H_1} (GeV)	98.29	115.17	125.34
m_{H_2} (GeV)	125.79	125.77	143.0
$R_{\gamma\gamma}$	1.12	1.144	1.363
R_{ZZ}	0.940	0.905	1.153

Table 3. Some specifics of the three benchmark points.

In the study of these benchmark points we therefore use a somewhat modified kinematical analysis. Specifically, all A_1 candidates (i.e., b-jet pairs, fat jets or τ-jet pairs) are required to be within 15 GeV off the (assumed known) A_1 mass. For each point we run two simulations, one for $H_1 \to A_1 A_1$ and one for $H_2 \to A_1 A_1$ and in each case the combined invariant mass of the two A_1 candidates is required to be within 30 GeV of the (assumed known) H_1 or H_2 mass.

The result of these studies are displayed in table 4, where the cross sections after all cuts are presented for the signal as well as the backgrounds. We also show the integrated luminosity needed to obtain $S/\sqrt{B} > 5$ with at least 10 events. The result of the jet substructure (fat jet) analysis is only shown for point 1 as this is the only scenario with an A_1 light enough for such studies to be useful, though, in that case, this is usually the most effective approach. Also, we do not include $H_1 \to A_1 A_1$ for point 3 as this channel is kinematically closed.

As stated before, the signals are in general larger than the backgrounds and, in many cases, the main constraint on the required luminosity is the requirement of at least 10 events. We also see in table 4 that WH is usually the most promising channel as it has the highest rates. It also has the highest backgrounds though, due to $t\bar{t}b\bar{b}$ and $t\bar{t}$ and, since these tend to increase with increasing H_i mass, we note that for $H_2 \to A_1 A_1$ in point 2 and 3 the VBF channel is somewhat better.

Comparing the detection prospects claimed for point 3 in table 4 in ZH and WH produc-

	Point 1				Point 2		Point 3
	$H_i = H_1$		$H_i = H_2$		$H_i = H_1$	$H_i = H_2$	$H_i = H_2$
	b-jets	fat jet	b-jets	fat jet	b-jets	b-jets	b-jets
$q\bar{q}H_i \to q\bar{q}2b2\tau$							
Signal [pb]	1.3×10^{-5}	7.0×10^{-6}	1.0×10^{-5}	1.3×10^{-5}	2.5×10^{-5}	1.6×10^{-5}	2.2×10^{-5}
$2j + 2b2\tau$	3.6×10^{-7}	1.2×10^{-7}	4.8×10^{-7}	3.0×10^{-7}	1.3×10^{-6}	1.8×10^{-6}	3.4×10^{-6}
$2j + t\bar{t}$	1.9×10^{-7}	1.9×10^{-7}	1.9×10^{-7}	3.7×10^{-7}	5.6×10^{-7}	9.4×10^{-7}	1.5×10^{-6}
$\mathcal{L}$ [fb^{-1}]	770	1400	970	750	390	630	460
$ZH_i \to 2\ell 4b$							
Signal [pb]	7.4×10^{-6}	7.9×10^{-6}	4.9×10^{-6}	7.7×10^{-6}	1.2×10^{-5}	6.3×10^{-6}	7.3×10^{-6}
$Z + 4b$ [pb]	1.4×10^{-6}	1.2×10^{-6}	1.5×10^{-6}	1.3×10^{-6}	3.1×10^{-6}	3.9×10^{-6}	4.0×10^{-6}
$\mathcal{L}$ [fb^{-1}]	1300	1300	2000	1300	860	2500	1900
$WH_i \to \ell 4b$							
Signal [pb]	5.2×10^{-5}	7.8×10^{-5}	3.4×10^{-5}	6.9×10^{-5}	8.2×10^{-5}	4.4×10^{-5}	4.9×10^{-5}
$W + 4b$ [pb]	1.6×10^{-6}	1.8×10^{-6}	1.5×10^{-6}	2.0×10^{-6}	2.4×10^{-6}	2.8×10^{-6}	2.3×10^{-6}
$t\bar{t}b\bar{b}$ [pb]	1.5×10^{-5}	1.3×10^{-5}	2.0×10^{-5}	1.8×10^{-5}	3.4×10^{-5}	4.6×10^{-5}	4.5×10^{-5}
$t\bar{t}$ [pb]	1.6×10^{-6}	4.8×10^{-7}	2.5×10^{-6}	7.8×10^{-7}	5.3×10^{-6}	7.9×10^{-6}	1.4×10^{-5}
$\mathcal{L}$ [fb^{-1}]	190	130	520	150	160	720	640

Table 4. Discovery prospects for the three benchmark points. $\mathcal{L}$ denotes the integrated luminosity required for a detection in the given channel.
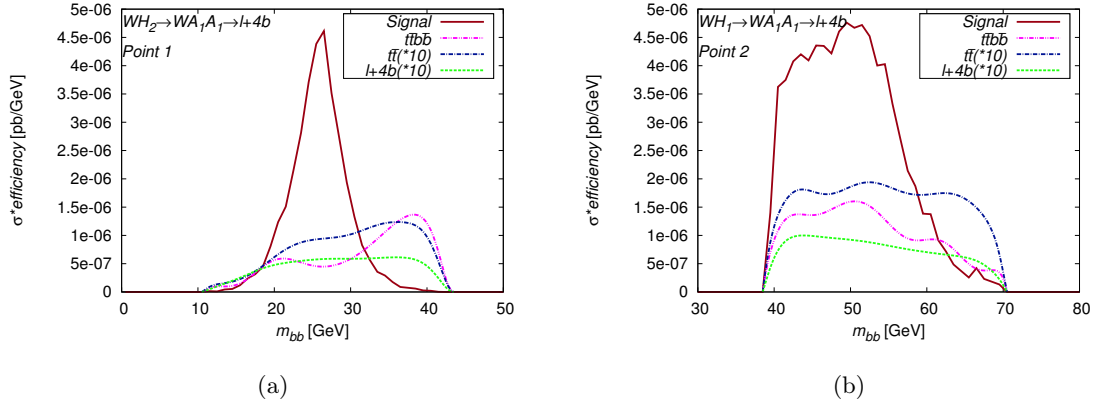

(a)   (b)

Figure 13. Signal and backgrounds for two of our benchmark points in the WH channel. The backgrounds have been smoothened for visual clarity and the $t\bar{t}$ and $\ell + 4b$ backgrounds have been multiplied by a factor 10 to be visible.

tion, with the reach shown in the corresponding plots (figures 9(b) and 11(b)), it is clear that the additional constraints on the kinematics due to the assumption about the mass spectrum are very important in improving sensitivity. This is especially true for WH as the $t\bar{t}b\bar{b}$ and $t\bar{t}$ backgrounds increase significantly with increasing overall invariant mass, hence rendering a (relatively low) cut on over all invariant mass very effective.

To illustrate more clearly the signal and backgrounds in the WH channels we plot these

as functions of the invariant mass of the b-jet pairs[6], m_{bb}, in figure 13 for $H_1 \to A_1 A_1$ in point 1 (figure 13(a)) and for $H_2 \to A_1 A_1$ in point 2 (figure 13(b)). Note that, due to the cuts in the analysis, the distributions are restricted to $m_{bb} \pm 15$ GeV and that both plots use single b-jet analysis only. In figure 13(a) it is clear that a somewhat narrower cut would significantly reduce the background from $t\bar{t}b\bar{b}$ without affecting the signal significantly. However, it is important to note that there are significant statistical uncertainties in the backgrounds (partially hidden by the smoothening) and this, together with the fact that the signal already dominates and that we do not include detector resolution, means that it is not clear how beneficial this cut really is.

From figure 13(b) we see that for heavier masses the invariant mass peak is smeared out towards smaller masses. That means that extending the allowed mass window downwards can increase the signal at the cost of larger backgrounds. A more detailed study including detector simulations would be necessary to properly optimise the invariant mass cuts but, as this is beyond the scope of this investigation, we leave that for future work.

9   Conclusions

In contrast to the more thoroughly studied MSSM, the NMSSM allows for the existence of very light Higgs scalars as well as pseudoscalars. Therefore, the discovery of, in particular, a light pseudoscalar Higgs state would not just prove the existence of physics beyond the SM but would also be inconsistent with minimal supersymmetry.

As arguably the NMSSM accommodates the 125 GeV Higgs more naturally than the MSSM, it is well worth a study. Although the most promising discovery channels of the aforementioned light pseudoscalar state are most likely based on GF production of heavier scalars that subsequently decay to $A_1 A_1$ or $A_1 Z$, we demonstrated here that also VBF and HS production of the heavier scalars can be accessible. Hence, these two additional production modes can well be exploited to study couplings not accessible in GF, such as those of the heavy scalars to SM gauge bosons. Especially encouraging is the fact that the most promising channels tend to be the ones starting with the non-SM-like scalar (i.e. H_2 for $H_1 = H_{\rm SM}$ and H_1 for $H_2 = H_{\rm SM}$); as these can have $\mathrm{BR}(H_i \to A_1 A_1)$ close to 1, the channels of this paper might be our only chance of measuring the couplings of these scalars to gauge bosons.

In these channels, the signal rates are substantially lower than in the case of GF, but the same is true for the backgrounds. Due to the nature of the couplings involved, the only decay chains of interest here are $H_{1,2} \to A_1 A_1$. For VBF production of $H_{1,2}$ the most promising of our final states is $2b2\tau$ (in addition to the two forward/backward jets), which may allow detection, certainly at 3000/fb but possibly also at 300/fb (albeit limited to the the $H_2 = H_{\rm SM}$ case).

For HS production, the background is even smaller, especially for the ZH mode. However, this channel also has a very small cross section and hence the signal will be very hard to extract.

---

[6]Included here are the two invariant masses of the first combination of b-jet pairs that have both invariant masses within $m_{A_1} \pm 15$ GeV.

As the event rates are indeed significantly smaller compared to VBF and GF, here it is most beneficial to employ the final state with the highest rate, i.e., $4b$.

Although still featuring a relatively low signal rate, WH production shows significantly better prospects than ZH. Despite significant backgrounds from $t\bar{t}b\bar{b}$ and $t\bar{t}$, the higher signal rates make this the most promising channel studied in this paper, at least for relatively light initial scalars. However, given the invariant mass structure of the main backgrounds, the signal tends to be overwhelmed unless one can cut on the four-b invariant mass and the enforced mass window needs to be relatively low. Therefore, the prospects for this channel diminish as the mass of the initially produced scalar increases, rendering VBF the most promising channel for heavier scalars.

In addition to general scans for sensitivity reach in parameter space, we have performed more detailed studies of three representative benchmark points. Here, we assumed knowledge of the masses of the produced scalar as well as the pseudoscalar (e.g., as measured in GF production) and used this information to constrain the kinematics. Especially for HS, this can dramatically improve the sensitivity, which, unless the produced scalar is too heavy, leads to detection via WH production already at less than 200/fb.

References

[1] U. Ellwanger, C. Hugonie, and A. M. Teixeira, *The Next-to-Minimal Supersymmetric Standard Model*, *Phys.Rept.* **496** (2010) 1–77, [arXiv:0910.1785].

[2] **ATLAS Collaboration**, G. Aad et al., *Observation of a new particle in the search for the Standard Model Higgs boson with the ATLAS detector at the LHC*, *Phys.Lett.* **B716** (2012) 1–29, [arXiv:1207.7214].

[3] **CMS Collaboration**, S. Chatrchyan et al., *Observation of a new boson at a mass of 125 GeV with the CMS experiment at the LHC*, *Phys.Lett.* **B716** (2012) 30–61, [arXiv:1207.7235].

[4] **CLEO Collaboration**, W. Love et al., *Search for Very Light CP-Odd Higgs Boson in Radiative Decays of Upsilon(S-1)*, *Phys.Rev.Lett.* **101** (2008) 151802, [arXiv:0807.1427].

[5] **E391a Collaboration**, Y. Tung et al., *Search for a light pseudoscalar particle in the decay $K_L^0 \to \pi^0\pi^0 X$*, *Phys.Rev.Lett.* **102** (2009) 051802, [arXiv:0810.4222].

[6] **BaBar collaboration**, J. Lees et al., *Search for di-muon decays of a low-mass Higgs boson in radiative decays of the $\Upsilon(1S)$*, *Phys.Rev.* **D87** (2013), no. 3 031102, [arXiv:1210.0287].

[7] **BaBar Collaboration**, J. Lees et al., *Search for a low-mass scalar Higgs boson decaying to a tau pair in single-photon decays of $\Upsilon(1S)$, Phys.Rev.* **D88** (2013), no. 7 071102, [arXiv:1210.5669].

[8] **BaBar Collaboration**, J. Lees et al., *Search for a light Higgs boson decaying to two gluons or $s\bar{s}$ in the radiative decays of $\Upsilon(1S)$, Phys.Rev.* **D88** (2013), no. 3 031701, [arXiv:1307.5306].

[9] **BABAR Collaboration**, I. Peruzzi, *Recent BABAR results on dark matter and light Higgs searches and on CP and T violation, EPJ Web Conf.* **71** (2014) 00108.

[10] **OPAL Collaboration**, G. Abbiendi et al., *Search for a low mass CP odd Higgs boson in e^+e^- collisions with the OPAL detector at LEP-2, Eur.Phys.J.* **C27** (2003) 483–495, [hep-ex/0209068].

[11] **ALEPH Collaboration**, S. Schael et al., *Search for neutral Higgs bosons decaying into four taus at LEP2, JHEP* **1005** (2010) 049, [arXiv:1003.0705].

[12] **D0 Collaboration**, V. Abazov et al., *Search for NMSSM Higgs bosons in the $h \to aa \to \mu\mu\mu\mu, \mu\mu\tau\tau$ channels using p anti-p collisions at $\sqrt{s} = 1.96$ TeV, Phys.Rev.Lett.* **103** (2009) 061801, [arXiv:0905.3381].

[13] **CMS Collaboration**, S. Chatrchyan et al., *Search for a light pseudoscalar Higgs boson in the dimuon decay channel in pp collisions at $\sqrt{s} = 7$ TeV, Phys.Rev.Lett.* **109** (2012) 121801, [arXiv:1206.6326].

[14] **CMS Collaboration**, S. Chatrchyan et al., *Search for a non-standard-model Higgs boson decaying to a pair of new light bosons in four-muon final states, Phys.Lett.* **B726** (2013) 564–586, [arXiv:1210.7619].

[15] **CMS Collaboration**, *Search for very light NMSSM Higgs boson produced in decays of a boson with mass near 125 GeV and decaying into tau-leptons*, Tech. Rep. CMS-PAS-HIG-14-019, CERN, Geneva, 2014.

[16] **CMS Collaboration**, *Search for an Higgs Like resonance in the diphoton mass spectra above 150 GeV with 8 TeV data*, Tech. Rep. CMS-PAS-HIG-14-006, CERN, Geneva, 2014.

[17] **CMS Collaboration**, *Search for di-Higgs resonances decaying to 4 bottom quarks*, Tech. Rep. CMS-PAS-HIG-14-013, CERN, Geneva, 2014.

[18] **ATLAS Collaboration**, G. Aad et al., *Search for Scalar Diphoton Resonances in the Mass Range $65 - 600$ GeV with the ATLAS Detector in pp Collision Data at $\sqrt{s} = 8\,TeV$, Phys.Rev.Lett.* **113** (2014), no. 17 171801, [arXiv:1407.6583].

[19] J. Dai, J. Gunion, and R. Vega, *Guaranteed detection of a minimal supersymmetric model Higgs boson at hadron supercolliders, Phys.Lett.* **B315** (1993) 355–359, [hep-ph/9306319].

[20] U. Ellwanger, *Higgs pair production in the NMSSM at the LHC, JHEP* **1308** (2013) 077, [arXiv:1306.5541].

[21] E. Accomando, A. Akeroyd, E. Akhmetzyanova, J. Albert, A. Alves, et al., *Workshop on CP Studies and Non-Standard Higgs Physics*, hep-ph/0608079.

[22] M. Almarashi and S. Moretti, *Low Mass Higgs signals at the LHC in the Next-to-Minimal Supersymmetric Standard Model, Eur.Phys.J.* **C71** (2011) 1618, [arXiv:1011.6547].

[23] M. Almarashi and S. Moretti, *Very Light CP-odd Higgs bosons of the NMSSM at the LHC in 4b-quark final states*, *Phys.Rev.* **D84** (2011) 015014, [arXiv:1105.4191].

[24] U. Ellwanger, J. F. Gunion, and C. Hugonie, *Difficult scenarios for NMSSM Higgs discovery at the LHC*, *JHEP* **0507** (2005) 041, [hep-ph/0503203].

[25] U. Ellwanger, J. F. Gunion, C. Hugonie, and S. Moretti, *Towards a no lose theorem for NMSSM Higgs discovery at the LHC*, hep-ph/0305109.

[26] U. Ellwanger, J. F. Gunion, and C. Hugonie, *Establishing a no lose theorem for NMSSM Higgs boson discovery at the LHC*, hep-ph/0111179.

[27] C. Hugonie and S. Moretti, *Higgs sector of nonminimal supersymmetric models at future hadron colliders*, *eConf* **C010630** (2001) P108, [hep-ph/0110241].

[28] A. Belyaev, S. Hesselbach, S. Lehti, S. Moretti, A. Nikitenko, et al., *The Scope of the 4 tau Channel in Higgs-strahlung and Vector Boson Fusion for the NMSSM No-Lose Theorem at the LHC*, arXiv:0805.3505.

[29] J. Forshaw, J. Gunion, L. Hodgkinson, A. Papaefstathiou, and A. Pilkington, *Reinstating the 'no-lose' theorem for NMSSM Higgs discovery at the LHC*, *JHEP* **0804** (2008) 090, [arXiv:0712.3510].

[30] A. Belyaev, J. Pivarski, A. Safonov, S. Senkin, and A. Tatarinov, *LHC discovery potential of the lightest NMSSM Higgs in the $h_1 \to a_1 a_1 \to 4$ muons channel*, *Phys.Rev.* **D81** (2010) 075021, [arXiv:1002.1956].

[31] S. Moretti and S. Munir, *Di-photon Higgs signals at the LHC in the next-to-minimal supersymmetric standard model*, *Eur.Phys.J.* **C47** (2006) 791–803, [hep-ph/0603085].

[32] S. Moretti, S. Munir, and P. Poulose, *Another step towards a no-lose theorem for NMSSM Higgs discovery at the LHC*, *Phys.Lett.* **B644** (2007) 241–247, [hep-ph/0608233].

[33] M. M. Almarashi and S. Moretti, *Muon Signals of Very Light CP-odd Higgs states of the NMSSM at the LHC*, *Phys.Rev.* **D83** (2011) 035023, [arXiv:1101.1137].

[34] U. Ellwanger and C. Hugonie, *Masses and couplings of the lightest Higgs bosons in the (M+1) SSM*, *Eur.Phys.J.* **C25** (2002) 297–305, [hep-ph/9909260].

[35] A. Djouadi, M. Drees, U. Ellwanger, R. Godbole, C. Hugonie, et al., *Benchmark scenarios for the NMSSM*, *JHEP* **0807** (2008) 002, [arXiv:0801.4321].

[36] F. Mahmoudi, J. Rathsman, O. Stål, and L. Zeune, *Light Higgs bosons in phenomenological NMSSM*, *Eur.Phys.J.* **C71** (2011) 1608, [arXiv:1012.4490].

[37] R. Dermisek and J. F. Gunion, *Escaping the large fine tuning and little hierarchy problems in the next to minimal supersymmetric model and $h \to aa$ decays*, *Phys.Rev.Lett.* **95** (2005) 041801, [hep-ph/0502105].

[38] J. F. Gunion, H. E. Haber, and T. Moroi, *Will at least one of the Higgs bosons of the next-to-minimal supersymmetric extension of the standard model be observable at LEP-2 or the LHC?*, *eConf* **C960625** (1996) LTH095, [hep-ph/9610337].

[39] B. A. Dobrescu, G. L. Landsberg, and K. T. Matchev, *Higgs boson decays to CP odd scalars at the Tevatron and beyond*, *Phys.Rev.* **D63** (2001) 075003, [hep-ph/0005308].

[40] U. Ellwanger, J. Gunion, C. Hugonie, and S. Moretti, *NMSSM Higgs discovery at the LHC*, [hep-ph/0401228](hep-ph/0401228).

[41] M. Lisanti and J. G. Wacker, *Discovering the Higgs with Low Mass Muon Pairs*, *Phys.Rev.* **D79** (2009) 115006, [arXiv:0903.1377].

[42] M. Almarashi and S. Moretti, *Reinforcing the no-lose theorem for NMSSM Higgs discovery at the LHC*, *Phys.Rev.* **D84** (2011) 035009, [arXiv:1106.1599].

[43] M. M. Almarashi and S. Moretti, *LHC Signals of a Heavy CP-even Higgs Boson in the NMSSM via Decays into a Z and a Light CP-odd Higgs State*, *Phys.Rev.* **D85** (2012) 017701, [arXiv:1109.1735].

[44] M. M. Almarashi and S. Moretti, *Scope of Higgs production in association with a bottom quark pair in probing the Higgs sector of the NMSSM at the LHC*, arXiv:1205.1683.

[45] S. King, M. Mühlleitner, R. Nevzorov, and K. Walz, *Discovery Prospects for NMSSM Higgs Bosons at the High-Energy Large Hadron Collider*, *Phys.Rev.* **D90** (2014) 095014, [arXiv:1408.1120].

[46] J. E. Kim, H. P. Nilles, and M.-S. Seo, *Singlet Superfield Extension of the Minimal Supersymmetric Standard model with Peccei-Quinn symmetry and a Light Pseudoscalar Higgs Boson at the LHC*, *Mod.Phys.Lett.* **A27** (2012) 1250166, [arXiv:1201.6547].

[47] S. Munir, L. Roszkowski, and S. Trojanowski, *Simultaneous enhancement in $\gamma\gamma$, $b\bar{b}$ and $\tau^+\tau^-$ rates in the NMSSM with nearly degenerate scalar and pseudoscalar Higgs bosons*, *Phys. Rev.* **D88** (2013) 055017, [arXiv:1305.0591].

[48] J. Kozaczuk and T. A. W. Martin, *Extending LHC Coverage to Light Pseudoscalar Mediators and Coy Dark Sectors*, arXiv:1501.0727.

[49] N.-E. Bomark, S. Moretti, S. Munir, and L. Roszkowski, *A light NMSSM pseudoscalar Higgs boson at the LHC redux*, *JHEP* **1502** (2015) 044, [arXiv:1409.8393].

[50] D. G. Cerdeno, P. Ghosh, and C. B. Park, *Probing the two light Higgs scenario in the NMSSM with a low-mass pseudoscalar*, *JHEP* **1306** (2013) 031, [arXiv:1301.1325].

[51] D. Curtin, R. Essig, and Y.-M. Zhong, *Uncovering light scalars with exotic Higgs decays to bbmumu*, arXiv:1412.4779.

[52] O. Stål and G. Weiglein, *Light NMSSM Higgs bosons in SUSY cascade decays at the LHC*, *JHEP* **1201** (2012) 071, [arXiv:1108.0595].

[53] D. Das, U. Ellwanger, and A. M. Teixeira, *Modified Signals for Supersymmetry in the NMSSM with a Singlino-like LSP*, *JHEP* **1204** (2012) 067, [arXiv:1202.5244].

[54] D. G. Cerdeño, P. Ghosh, C. B. Park, and M. Peiró, *Collider signatures of a light NMSSM pseudoscalar in neutralino decays in the light of LHC results*, *JHEP* **1402** (2014) 048, [arXiv:1307.7601].

[55] S. King, M. Mühlleitner, R. Nevzorov, and K. Walz, *Natural NMSSM Higgs Bosons*, *Nucl.Phys.* **B870** (2013) 323–352, [arXiv:1211.5074].

[56] N.-E. Bomark, S. Moretti, S. Munir, and L. Roszkowski, *Revisiting a light NMSSM pseudoscalar at the LHC*, arXiv:1412.5815.

[57] N.-E. Bomark, S. Moretti, S. Munir, and L. Roszkowski, *A light NMSSM pseudoscalar Higgs boson at the LHC Run 2*, arXiv:1502.0576.

[58] D. Curtin, R. Essig, S. Gori, P. Jaiswal, A. Katz, et al., *Exotic decays of the 125 GeV Higgs boson*, *Phys.Rev.* **D90** (2014), no. 7 075004, [arXiv:1312.4992].

[59] U. Ellwanger, *A Higgs boson near 125 GeV with enhanced di-photon signal in the NMSSM*, *JHEP* **1203** (2012) 044, [arXiv:1112.3548].

[60] S. King, M. Mühlleitner, and R. Nevzorov, *NMSSM Higgs Benchmarks Near 125 GeV*, *Nucl.Phys.* **B860** (2012) 207–244, [arXiv:1201.2671].

[61] U. Ellwanger and C. Hugonie, *Higgs bosons near 125 GeV in the NMSSM with constraints at the GUT scale*, *Adv.High Energy Phys.* **2012** (2012) 1, [arXiv:1203.5048].

[62] T. Gherghetta, B. von Harling, A. D. Medina, and M. A. Schmidt, *The Scale-Invariant NMSSM and the 126 GeV Higgs Boson*, *JHEP* **1302** (2013) 032, [arXiv:1212.5243].

[63] J. Cao et al., *A SM-like Higgs near 125 GeV in low energy SUSY: a comparative study for MSSM and NMSSM*, *JHEP* **1203** (2012) 086, [arXiv:1202.5821].

[64] M. Badziak, M. Olechowski, and S. Pokorski, *New Regions in the NMSSM with a 125 GeV Higgs*, *JHEP* **1306** (2013) 043, [arXiv:1304.5437].

[65] F. Feroz, M. Hobson, and M. Bridges, *MultiNest: an efficient and robust Bayesian inference tool for cosmology and particle physics*, *Mon.Not.Roy.Astron.Soc.* **398** (2009) 1601–1614, [arXiv:0809.3437].

[66] http://www.th.u-psud.fr/NMHDECAY/nmssmtools.html.

[67] P. Bechtle, O. Brein, S. Heinemeyer, G. Weiglein, and K. E. Williams, *HiggsBounds: Confronting Arbitrary Higgs Sectors with Exclusion Bounds from LEP and the Tevatron*, *Comput.Phys.Commun.* **181** (2010) 138–167, [arXiv:0811.4169].

[68] P. Bechtle, O. Brein, S. Heinemeyer, G. Weiglein, and K. E. Williams, *HiggsBounds 2.0.0: Confronting Neutral and Charged Higgs Sector Predictions with Exclusion Bounds from LEP and the Tevatron*, *Comput.Phys.Commun.* **182** (2011) 2605–2631, [arXiv:1102.1898].

[69] P. Bechtle, O. Brein, S. Heinemeyer, O. Stål, T. Stefaniak, et al., *Recent Developments in HiggsBounds and a Preview of HiggsSignals*, *PoS* **CHARGED2012** (2012) 024, [arXiv:1301.2345].

[70] P. Bechtle, O. Brein, S. Heinemeyer, O. Stål, T. Stefaniak, et al., HiggsBounds − 4: *Improved Tests of Extended Higgs Sectors against Exclusion Bounds from LEP, the Tevatron and the LHC*, *Eur.Phys.J.* **C74** (2014) 2693, [arXiv:1311.0055].

[71] A. Arbey and F. Mahmoudi, *SuperIso Relic: A program for calculating relic density and flavor physics observables in Supersymmetry*, *Comput.Phys.Commun.* **176** (2007) 367–382, [arXiv:0906.0369].

[72] **Particle Data Group**, J. Beringer et al., *Review of Particle Physics (RPP)*, *Phys.Rev.* **D86** (2012) 010001.

[73] **Planck Collaboration**, P. Ade et al., *Planck 2013 results. XVI. Cosmological parameters*, *Astron.Astrophys.* **571** (2014) A16, [arXiv:1303.5076].

[74] G. Belanger, F. Boudjema, A. Pukhov, and A. Semenov, *microOMEGAs2.0: a program to calculate the relic density of dark matter in a generic model*, *Comput.Phys.Commun.* **181** (2010) 1277–1292, [`hep-ph/0607059`].

[75] *Precise determination of the mass of the higgs boson and studies of the compatibility of its couplings with the standard model*, Tech. Rep. CMS-PAS-HIG-14-009, CERN, Geneva, Jul, 2014.

[76] **ATLAS Collaboration**, G. Aad et al., *Measurement of Higgs boson production in the diphoton decay channel in pp collisions at center-of-mass energies of 7 and 8 TeV with the ATLAS detector*, *Phys.Rev.* **D90** (2014), no. 11 112015, [`arXiv:1408.7084`].

[77] **ATLAS Collaboration**, G. Aad et al., *Measurements of Higgs boson production and couplings in the four-lepton channel in pp collisions at center-of-mass energies of 7 and 8 TeV with the ATLAS detector*, *Phys.Rev.* **D91** (2015), no. 1 012006, [`arXiv:1408.5191`].

[78] **ATLAS Collaboration**, G. Aad et al., *Observation and measurement of Higgs boson decays to WW^* with the ATLAS detector*, `arXiv:1412.2641`.

[79] *Updated coupling measurements of the higgs boson with the atlas detector using up to $25\,fb^{-1}$ of proton-proton collision data*, Tech. Rep. ATLAS-CONF-2014-009, CERN, Geneva, May, 2014.

[80] **ATLAS**, G. Aad et al., *Measurement of the Higgs boson mass from the $H \to \gamma\gamma$ and $H \to ZZ^* \to 4\ell$ channels with the ATLAS detector using $25\,fb^{-1}$ of pp collision data*, *Phys.Rev.* **D90** (2014), no. 5 052004, [`arXiv:1406.3827`].

[81] J. Alwall, R. Frederix, S. Frixione, V. Hirschi, F. Maltoni, et al., *The automated computation of tree-level and next-to-leading order differential cross sections, and their matching to parton shower simulations*, *JHEP* **1407** (2014) 079, [`arXiv:1405.0301`].

[82] T. Sjöstrand, S. Mrenna, and P. Z. Skands, *A Brief Introduction to PYTHIA 8.1*, *Comput.Phys.Commun.* **178** (2008) 852–867, [`arXiv:0710.3820`].

[83] M. Cacciari, G. P. Salam, and G. Soyez, *FastJet User Manual*, *Eur.Phys.J.* **C72** (2012) 1896, [`arXiv:1111.6097`].

[84] **LHC Higgs Cross Section Working Group**, S. Dittmaier et al., *Handbook of LHC Higgs Cross Sections: 1. Inclusive Observables*, `arXiv:1101.0593`.

[85] J. M. Butterworth, A. R. Davison, M. Rubin, and G. P. Salam, *Jet substructure as a new Higgs search channel at the LHC*, *Phys.Rev.Lett.* **100** (2008) 242001, [`arXiv:0802.2470`].

[86] M. Carena, T. Han, G.-Y. Huang, and C. E. Wagner, *Higgs Signal for $h \to aa$ at Hadron Colliders*, *JHEP* **0804** (2008) 092, [`arXiv:0712.2466`].

[87] K. Cheung, J. Song, and Q.-S. Yan, *Role of $h \longrightarrow eta\ eta$ in Intermediate-Mass Higgs Boson Searches at the Large Hadron Collider*, *Phys.Rev.Lett.* **99** (2007) 031801, [`hep-ph/0703149`].

[88] J. Cao, F. Ding, C. Han, J. M. Yang, and J. Zhu, *A light Higgs scalar in the NMSSM confronted with the latest LHC Higgs data*, *JHEP* **1311** (2013) 018, [`arXiv:1309.4939`].